Cloverleaf interchange boundary extraction from airborne LiDAR data based on advanced neighborhood structure and contour analysis

CHEN Zhuo[1], MA Hongchao[1,2], ZHANG Liang[1]

1. *School of Remote Sensing and Information Engineering, Wuhan University, Wuhan* 430079, *China*;
2. *State Key Laboratory of Information Engineering in Surveying, Mapping and Remote Sensing, Wuhan University, Wuhan* 430079, *China*

Abstract: It is difficult to detect city cloverleaf, which is arised from shortcomings in traditional remote sensing image and the lack of appropriate methods. This paper presents an effective approach to extract city cloverleaf interchange footprints and boundary based on laser scanning data. We developed a plane-based approach to segment the data in the profile area and built a point o rganization structure called advanced scanline profile neighborhood system to identify the seed points. Alpha-shape algorithm was introduced to segment the seed points and generate the point sets boundaries. The cloverleaf interchange boundary was located by three-dimensional contour analysis based on model description. The complete cloverleaf footprints were determined by region-growing algorithm in the end, and meanwhile, the final cloverleaf boundary was obtained. The experiment was performed on the LiDAR data collected on a urban city. The result shows integrity and validly of our function that can get accurate length, width and morphology measurements comparing with the manual measurements from the high resolution ortho image.

Key words: urban cloverleaf interchange, LiDAR, scanline profile neighborhood structure, Alpha-shape algorithm

CLC number: P237 **Document code:** A

Citation format: **Chen Z, Ma H C and Zhang L. 2013. Cloverleaf interchange boundary extraction from airborne LiDAR data based on advanced neighborhood structure and contour analysis. Journal of Remote Sensing, 1 7(5): 1146 – 1157 [DOI: 10.11834/jrs.20131213]**

1 INTRODUCTION

Urban cloverleaf interchange is the multi-level three-dimensional land-form structure which consists of the bridge deck, space intersection and space connection. It is an important part of the urban traffic and the most complicated section of urban road (Chen, et al., 2000; Li, 2011). Research on urban traffic has been long based on acquisition and reconstruction of the road information, while the information extraction of urban cloverleaf i nterchange is limited. Therefore, the information extraction of urban cloverleaf interchange from remote sensing data needs e ffective methods.

Traditional road research includes the extraction of road pixels, road edges and estimation of road parameters (orientation, width, the center line) from images or other data source through automatic or semi-automatic methods (Hu & Tao, 2007; Zhang, e t al., 2008; Poullis & You, 2010; Lin, 2012). However, although the cloverleaf interchange has certain similar characteristics of the road, it also has a multi-level space complex structure, so that the two-dimensional method of road recognition and judgment cannot solve the problem. Zhang try to reconstruct three-dimensional road network by stereo mapping and knowledge based i mage analysis, but the process is complex and is not the reconstruction of multi-level structure(Zhang, 2004). As a preliminary a ttempt of three-dimensional road visualization, Zuo build three-dimensional road model by projecting two-dimensional road p rofile into co-registered DTM to get the height values of the points on road edge, however the localization and expression of line and planar in three-dimensional environment are not m entioned in his paper (Zuo, et al., 2004). Airborne LiDAR s ystem obtains fast development in past decades, which is capable of providing high-density point cloud of the area in a short time (Ackermann, 1999), provides a good condition for a cquiring information on complex three-dimensional geographic object. In the field of urban traffic research, there have been some methods based on LiDAR data (Zhu, et al., 2004; Clode, et al., 2006). Vosselman (2003) proposed methods of three-dimensional geographic object information extracting by updating two-dimensional structure reconstruction with LiDAR data, he also put forward a variety of three-dimensional reconstruction algo-

Received: 2011-08-15; **Accepted:** 2013-03-25; **Version of record first published:** 2013-04-02

Foundation: National Science and Technology and Ministry (No. 2012BAH34B02); Wuhan University Doctroal Candidate Independent Research (No. 2013213020203)

First author biography: CHEN Zhuo (1985—), male, Ph. D. candidate, he majors in LiDAR data processing and three-dimensional modeling technology. E-mail: zchen0916@whu.edu.cn

Corresponding author biography: MA Hongchao (1969—), male, professor. His research interest are LiDAR data processing and application, remote sensing image processing and geostatistics. E-mail: hchma@whu.edu.cn

rithms for modeling of roads and trees in urban areas based on the edge information in cadastral. Following his idea, Oude E lberink completed the reconstruction of three-dimensional multi-level roads with LiDAR and cadastral map. (Oude Elberink &Vosselman 2009) . But in his algorithm, a lot of planar segmentation and fitting were employed, which needs a great amount of calculation, his road detection method based on linear feature d etection was not suitable in large curvature structure of the c loverleaf interchange.

This paper presents a method of abstracting large-scale c loverleaf interchange from LiDAR point clouds, which acquires cloverleaf interchange feet point and its outline from urban c ompact district data, constructs an advanced scanline profile neighborhood structure based on dispersed point clouds, separates point set belongs to different surface features. These approaches thus form multiple independent connection sections, and identify cloverleaf interchange through abstracting and a nalyzing seed points three-dimensional outline.

2 METHOD

In the city, both the main body of cloverleaf interchange and the ramps rise above the bare earth, both of which have big elevation change. In our method, the advanced point neighborhood system helps to detect and extract multi-level structures, and the detection is less sensitive to the object's geometry characteristics. Therefore, it is suitable for cloverleaf interchange detection. After selecting the seed points, Alpha-shape a lgorithm is introduced to segment the seed point sets and get their high precision outlines. The seed points are screened and the outline of cloverleaf interchange is selected. We complete the extraction of cloverleaf interchange by finishing the extraction of points in the connections between cloverleaf interchange and the bare earth using region-growing algorithm. The entire workflow of our method is shown in Fig. 1.

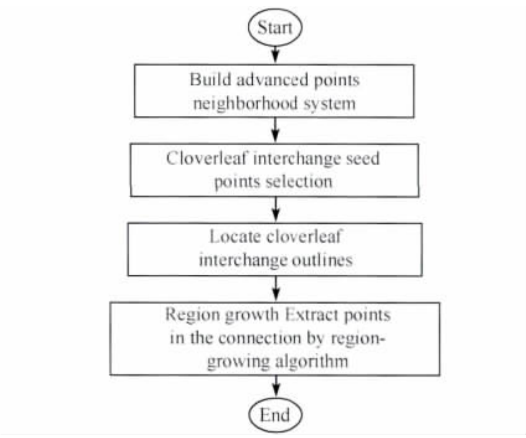

Fig. 1 workflow of our method

2.1 Advanced point profile neighborhood system

The effective point neighborhood system is the vital part and foundation of calculation, and it is the primary task to establish the point neighborhood relationship(Filin & Pfeifer 2005) . The common forms of point neiborhood system, like regular grid or Triangulated Irregular Network(TIN) lost precision of points and could not express the topology.

The profile tool is a common data-processing tool, which projects points in the narrow area to the vertical plane and checks the terrain rises and falls. Sithole suggests establish profile-based point neighborhood system with such idea(Sithole & Vosselman 2005) . It is to cover the points by scanning-line, and to set the range of the scanning-line as the profile area within ordered points. The point-to-point neighborhood relationship is established according to the value of slope threshold (Fig. 2) . The divided point section is called line segment, e. g. L_1. The whole points are scanned in different directions (normally in horizontal direction, in vertical direction and in the direction with the slope of 45°) , they are segmented, and multi-directional s egmentation results from different independent connection s ections. The multi-directional scanline profile tool can achieve good results while applying to laser points filtering, and the result of the segmentation are independent of the surface condition, however, the unitary value of slope threshold can lead to the wrong segmentation in several cases, like L_1, L_3 in Fig. 2. This will influence the processing of the subsequent calculation.

In the point sets of the profile, the points of different surface features are on different planes, so they have different values of slope. In addition, the densities among points are d ifferent. In order to avoid error segmentation, the advanced plane-based method and advanced point neighborhood system are proposed in this paper. Our method checks the straight lines of various slopes in the profile, while judging in light of densities, combining the neighborhood regions with gentle slopes, and establishes advanced point neighborhood structure according to the scanning-lines in various directions. Compared with the previous system, the advanced neighborhood system can precisely express the subordinate relationships between points and the surface features (as for many irregular surface features, such as buildings with gabled roof, like L_6, L_7 in Fig. 3) . At the same time, the error segmentation in the profile can be avoided. The visualization of those different points neighborhood system we discussed are shown in Fig. 4. The process of building our a dvanced points neighborhood system are as below

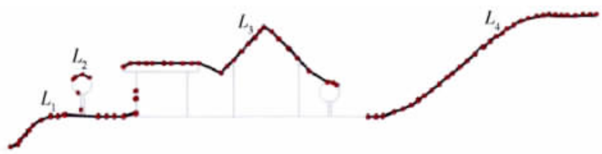

Fig. 2 The segmentation by the slope threshold values

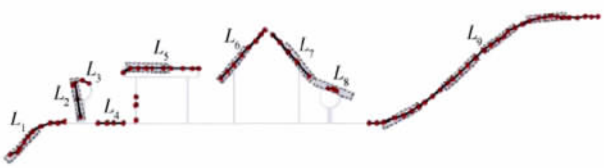

Fig. 3 The segmentation by our local plane-based function

(1) Get the points in one profile, the points are sorted by $X' = x\sin\theta + y\cos\theta$(x, y are points coordinates, θ is the direction for the scan-line) . For any point P_i(i is the index of point) , calculate the slope of P_i and its previous point P_{i-1}, slope $S(P_{i-1}, P_i) = \arctan\left(\frac{z_i - z_{i-1}}{\sqrt{(x_i - x_{i-1})^2 + (y_i - y_{i-1})^2}}\right)/\pi$, calculate the distribution of slope values by histogram, the interval of the histogram is $5/\pi$. Points in different intervals are put into different collection $\boldsymbol{G}_i = \{P_0, \cdots, P_i\}$.

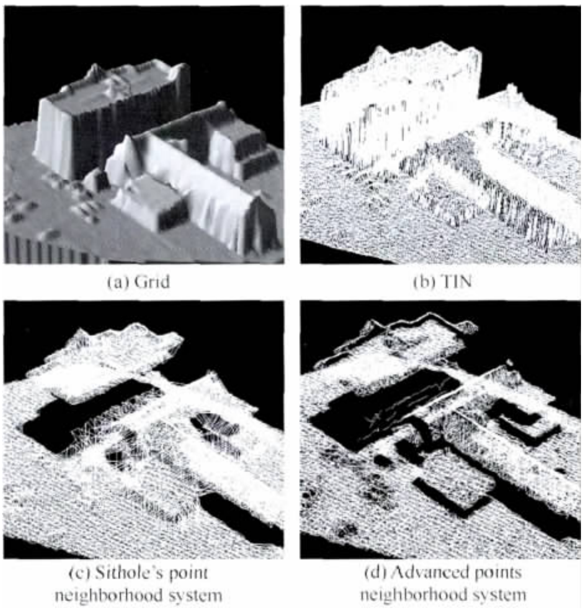

Fig. 4 Visualization of different points neighborhood system

(2) Get $\boldsymbol{G}_i$ in the profile, which the number of points is bigger than 2. Select P_j at random, if $P_{j-1}, P_{j+1} \in \boldsymbol{G}_i$, take $\{P_{j-1}, P_j, P_{j+1}\}$ as the starting point for the line segment L_1, connect the neighborhood point and calculate the average point distance D_{a1}, the variance of point distance is δ_1 and the average slope is S_{a1}, a straight line l_1 is fitted with the least square method based on the points of L_1.

(3) Construct a space cylinder region whose radius is R and take L_1 as its central axis, search for one front point and one rear point P_{j-2} and P_{j+2} at both ends. If the distance $|D_{j-2,j-1} - D_{a1}| < 3\delta_1$ (or $|D_{j+1,j+2} - D_{a1}| < 3\delta_1$) and P_{j-2} (or P_{j+2}) falls into the cylinder region, add P_{j-2} (or P_{j+2}) to the line segment L_1, update the value of average point distance and invariance δ_1, fit the straight Line l_1 again. If P_{j-2} (or P_{j+2}) do not satisfy the above properties, make the same judgment on P_{j-3} (or P_{j+3}) and add it to the line segment, take P_{j-2} (or P_{j+2}) as isolated point; otherwise, stop the search of this end. Having finished the growing of the line segment L_1, e liminate the points of L_1 out from $\boldsymbol{G}_i$, and search for new line segments. Repeat (3) until the number of the rest points in G_i is less than 2.

(4) Go through all the line segments in the profile, if for the two neighboring line segments L_i and L_j, if the distance between the end point of L_i and the starting point of L_j satisfies the condition: $D_{ei,bj} < \max(D_{ai}, D_{aj}) + 3\max(\delta_i, \delta_j)$, calculate the similar coefficient $\text{sim}_{i,j} = \frac{1}{1 + \sqrt{(D_{ai} - D_{aj})^2 + \beta(S_{ai} - S_{aj})^2}}$, β is a regnlation parameter, if its is larger than predefined threshold $\min_{\text{sim}}$, merge L_i and L_j as one line. Repeat (4) till there are no neighboring line segments to be combined.

2.2 Seed points extraction

According to the various characteristics of the city cloverleaf and the features of LIDAR, we describe the cloverleaf as below.

(1) The cloverleaf interchange is spatially the three-dimensional space extension of the city roads. The main bridge and the branch roads are all above the bare earth. (2) Huge cloverleaf i nterchange normally crosses very long distance of road, so in its region, the length of the existing line segment should be larger than the other surface features, such as the building and the v egetation. (3) The connection between terminal points of the main bridge and the end of the ramps and the connections with the bare earth should be gentle, and the bridge direction of the connections should be parallel to road direction (Fig. 5).

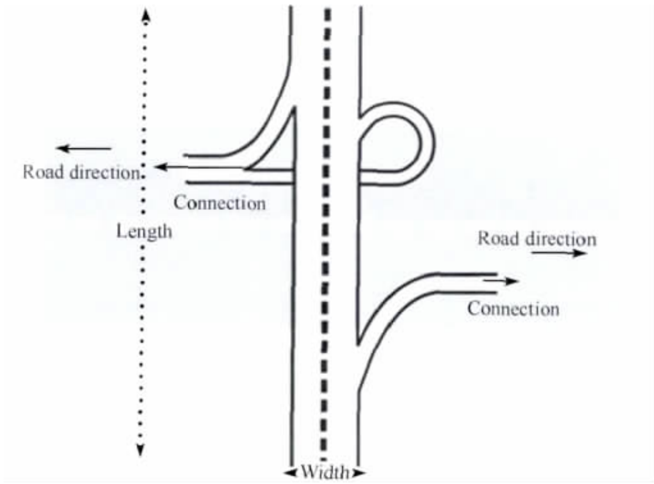

Fig. 5 Model for cloverleaf interchage

Based on the point neighborhood system built in Section 2.1, and according to model description (1), we collect the seed point from the point statistics as below.

First, define the threshold of the height difference Δ_{upper}. Then select the set of line segments from one profile $\{L_1, L_2, \cdots, L_i\}$. If the height H_{P_i} of each point L_i, compared with the a verage point height of the neighboring line segments $H_{L_{i-1}}, H_{L_{i+1}}$, satisfies the formula $H_{P_i} - \min(H_{L_{i-1}}, H_{L_{i+1}}) > \Delta_{\text{upper}}$, L_i is tagged as the upper line segment. Is for a line segment L_j adjacent to an upper line segment L_i, the average point height of L_j have $|H_{L_i} - H_{L_j}| < \Delta_{\text{upper}}$, L_j is also tagged as upper line segment. Finally for each point P_i in the las file $\boldsymbol{N}_{\text{LAS}}(P)$, calculate the number of u pper line segments through the point in different directions $Num_{\text{upper}}(\boldsymbol{G}_i)$, define $Num_{\text{upper}}(\boldsymbol{G}_i)$ the total number of line segments through P_i, the seed point set can be chose by $\boldsymbol{N}_{\text{Seed}}(P) = \{P_i \in \boldsymbol{N}_{\text{LAS}}(P) \mid Num_{\text{upper}}(\boldsymbol{G}_i) \leqslant Num(G_i)/2\}$. Point 1, point 3, point 4, point 5 (Fig. 6), the calculating approach can be applied to multi-layer structure (point 5) and it can also be applied to surface features with various geometry (point 1, point 3, point 4).

2.3 Seed points filtering and complete cloverleaf interchange footprints extraction

In seed point sets, the filtering of the seed points should be conducted through the analysis of the point sets′ outlines c ombined with the description of the model of cloverleaf interchange. However, for scattered points, the conventional convex hull calculation methods cannot give precise vector of its outlines, and cannot do segmentation among the points in different independent sections (Fig. 7(a)). This has hindered the further processing of the calculation. In this paper, Alpha-shape algorithm is introduced to calculate the point sets′ precise outline vectors, and a filtering process based on cloverleaf interchange model description is than conducted, which has secured the correct location of the cloverleaf.

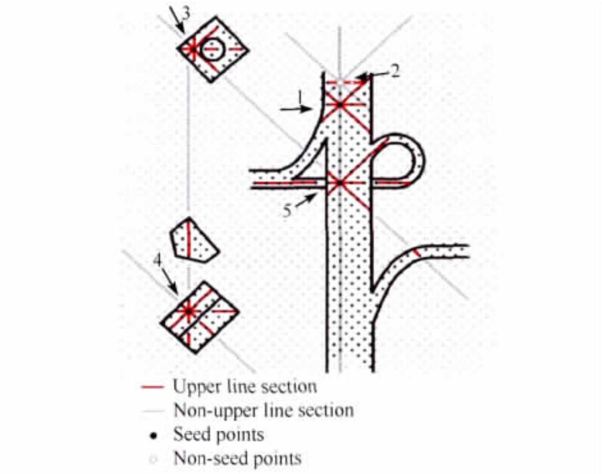

Fig.6 Seed point selection

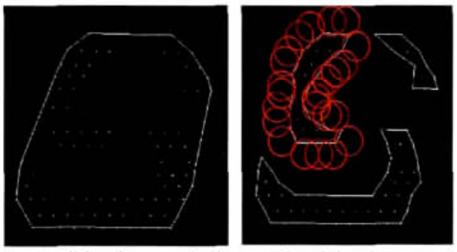

(a) Traditional convex hull (b) Alpha-shape

Fig.7 The outline of the seed points

Alpha-shape algorithm is efficient for outline reconstruction from scattered points. We can imagine that a circle with α radius is rolling around the points. When α value is big enough, the c ircle will not fall into the area of accumulated points. The rolling track will form the boundary of these discrete points. Contrarily, when α value is very small, every point might be the boundary. When the α value is approaching infinity, Alpha-shape will be the convex hull (Shen, et al., 2008). Alpha-shape algorithm satisfies our need for seed points fitering. The stages of the process include:

(1) Isolate the seed points from the non seed points, the noise and outliers are removed by K-means clustering and the connection between points.

(2) Use Alphas-shape algorithm to obtain the outlines of different sets of seed points: $\boldsymbol{\alpha}$-***Shape*** $= \{\boldsymbol{A}_1, \boldsymbol{A}_2, \cdots, \boldsymbol{A}_n\}$, $\boldsymbol{A}_i$ is a polygon vector.

(3) $\boldsymbol{A}_i$ is a polygon vector which consist of a set of edges connected with the beginning and the end: $\boldsymbol{A}_i = \{E_1, E_2, \cdots, E_n\}$.

We classify the edges E_i into two classes by calculating high difference of the points H_{Diff} in two rectangle buffer zones at both sides of E_i (Fig. 8), the threshold is Δ_{junc}, if $H_{\mathrm{Diff}} < \Delta_{\mathrm{junc}}$, tag E_i as Junction edge, if not tag it as Common edge.

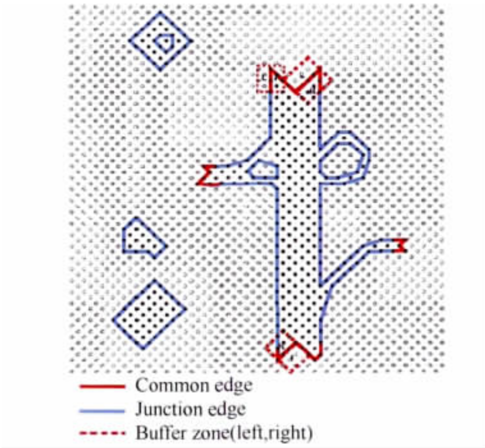

Fig. 8 Cloverleaf interchange outline detecting

(4) The outlines without Junction edge should be ruled out from the location of clovereleaf interchage (Fig. 8), in the remaining, according to model description (2), the outline within the longest line segments should be located and take as the outline of the cloverleaf points, and all the points inside are labeled as the initial cloverleaf points.

In the initial points, most cloverleaf footprints have been collected, but the connections with surfaces of the bare earth are not completed, because the points of the line segments in some directions are connected with the earth surface, and they do not belong to the upper line segment. The final complete cloverleaf interchange points are collected by region increase approach. Find the end points of the Junction edge in the outline and label them as the initial points of the region growth.

For the initial point P, get the lengths of the line segments through the point, and take the direction of the max-length line segments as the direction of the road, which is also the growth direction. Obtain the successive point P_i of the line segments in the direction. Set the front point and the rear point as the centre, fit lines $line_{i-}$, $line_{i+}$, and compare the differences $Diff_-$, $Diff_+$ (the distance between local points, usually three local points and $line_{i-}$, $line_{i+}$ (Fig. 9). If $Diff_- \leqslant Diff_+$, add it to the point set of the cloverleaf interchange. Repeat the process till the point that does not meets the inequality formula.

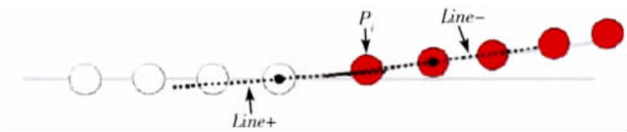

Fig. 9 The region growth in the line section in road direction

3 EXPERIMENT AND ANALYSIS

In order to testify the feasibility of our method, we chose laser point cloud collected in 2009 at Nanning, in Guangxi Province, as our experimental data. The experiment data collects from dense urban district, which includes large-scale cloverleaf interchange, various urban surface features (Fig. 10(a)). We design and implement our algorithm model in self-dependent development ALDpro software platform. After experiment and testify, it is proven that adopts the following parameter values can acquire satisfying result (Table 1). The threshold for estimating upper line segment and Junction edge can be set by manual, the result will not changed much if these two values have shifted in a small range, the value of parameter α should be greater than average point distance.

Table 1 Algorithm parameter

Parameter	Description	Values
min_{sim}	Line segments similarity threshold	0.74
β	Accommodation parameter in similarity calculation	0.11
Δ_{upper}	Upper line estimation threshold	2.47 m
Δ_{junc}	Junction edge estimation threshold	1.52 m
α	Alpha-shape parameter	2.8 m

Fig. 10(b) shows the result of seed points extraction, the seed points includes cloverleaf interchange footprints, there are also points from building, vegetation surfaces and so on, we can see that the points neighborhood system we built performs good for seed points extraction. Fig. 11(a) shows the outlines of different seed point sets gained by Alphas-shape algorithm after getting rid of noise and outlier of points, and this method can separate the seed points subset and acquire its outline accurately.

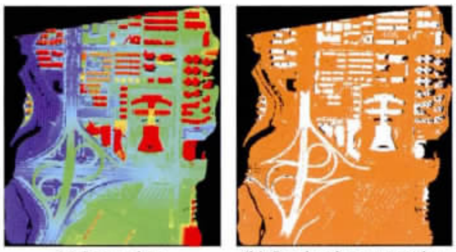

(a) Laser data (b) Seed points extraction

Fig.10 Seed points selection

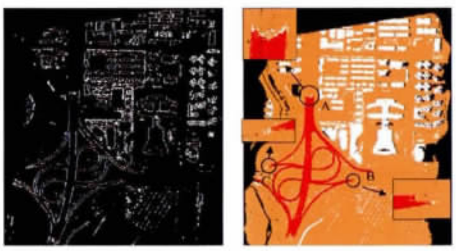

(a) Outlines of different seed points sets (b) Cloverleaf interchange points (red)

Fig.11 Cloverleaf interchange points extraction

Fig. 11(b) shows the location of cloverleaf interchange after screening the outlines, includes the points of main cloverleaf interchange and all of the ramps, but some regions (A,B,C in Fig. 11(b)) are incomplete, Fig. 12(a) shows the complete result after region growth process. Fig. 12 (b) shows its outlines.

To validate the completeness and correctness of our cloverleaf interchange extraction method, this paper makes comparison with the manual classification result. The number of cloverleaf interchange point obtained by our method is 42367; while the manual result is 44352. The completeness of our method is 92.94%. In addition, the rate of the true positive points we lost is 4.47%, which mainly dues to the incomplete extraction of points in the connection between cloverleaf and the bare earth. The ratio of false negative points that were wrongly extracted is 2.75%, which dues mainly to the few vehicle points which are moving on bridges. We also overlao the cloverleaf interchange outline we get with ortho image (0.3 m resolution) (Fig. 13). By comparison, a finding can be seen, that is, in most areas, the o utline that is obtained differs one or two pixels of the edge of the i dentified one in the ortho image. This mainly comes from the difference between point cloud samples and image grids itself. In the local area (Fig. 13(b)), due to the tree shelter, lower points density, and data holes, the difference is about three or four pixels.

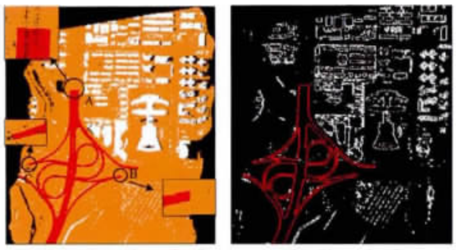

(a) Complete cloverleaf interchange footprints (b) Cloverleaf interchange outline

Fig.12 complete cloverleaf interchange footprints extraction

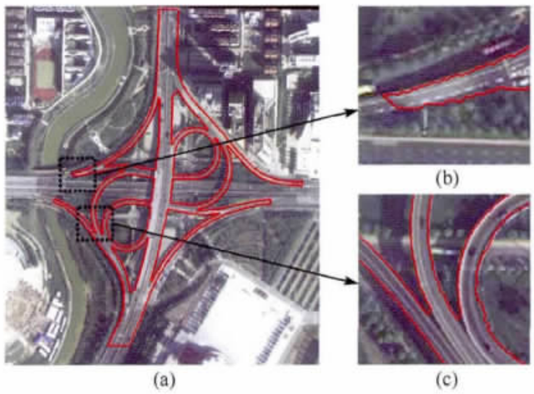

Fig.13 Overlap the outline of cloverleaf interchange with ortho-image

Other reasons that affect extraction correctness mainly includes: because the few handrail point of the bridge floor edge and points from isolation belt of the main bridge center in the middle, using the method of this place has great difference with surrounding height, they are seen as outliers elimination. Holes on the edge of dates affect in some degree the algorithm of region growth; there are many data points on the wall. Because they have the same X coordinate value, sorting in the profile cannot be done. This leads to the wrong segmentation of wall point set.

4 CONCLUSION

This paper presents a method for extracting cloverleaf interchange footprints and its outline from airborne laser scanner data with height precision. First, an plane-based profile points s egmentation method is proposed to build advanced points neighborhood system, it provides detail segmentation of point sets from different surfaces and objects, avoids mistakes made by single slope judgment, and obtains the seed points of cloverleaf interchange. Then, this paper seed points screening is performed by locating the cloverleaf interchange outline generated by Alpha-shape algorithm, which can obtain its irregular outline e xactly, and raises the accuracy of location. Experiment proves that using the method of this paper to obtain cloverleaf interchange footprints has higher completeness and precision. It's practical and effective. Its result can play great importance in cloverleaf interchange designing, digital city construction and traffic information management. What need to be improved are the correctness and completeness of extraction points in the c onnection between the cloverleaf interchange and the bare earth. The process of detection of points from bridge vehicles needs to be added in, so rate of false negative points extracted can be d ecreased further. Furthermore, effective line simplified algorithm of cloverleaf interchange outlines is needed to be studied, so rags and serious sunken of outlines can be eliminated.

REFERENCES

Ackermann F. 1999. Airborne laser scanning-present status and future e xpectations. ISPRS Journal of Photogrammetry and Remote Sensing, 54(2/3): 64-67 [DOI: 10.1016/S0924-2716(99)00009-X]

Chen J, Sun M and Zhou Q M. 2000. Expression and visualization of cloverleaf junction in a 3-dimensional city model. GeoInformatica, 4(4): 375-386 [DOI: 10.1023/A:1026513912425]

Clode S, Rottensteiner F, Kootsookos P J and Zelniker E E. 2006. Detection and vectorisation of roads from lidar data. Photogrammetric E ngineering & Remote Sensing, 2006

Filin S and Pfeifer N. 2005. Neighborhood systems for airborne laser data. Photogrammetric Engineering & Remote Sensing, 71(6): 743-755

Hu X and Tao V. 2007. Automatic extraction of main road centerlines from high resolution satellite imagery using hierarchical grouping. Photogrammetric Engineering and Remote Sensing, 73: 1049-1056

Li H. 2011. Road extraction and modeling with LiDAR and RS image in urban area. Acta Geodaetica Et Cartographica Sinica, 40(1): 133

Lin X G. 2012. Methods of road tracking from high resolution remotely sensed imagery. Acta Geodaetica et Cartographica Sinica, 41(4): 631

Oude Elberink S J and Vosselman G. 2009. 3D information extraction from laser point clouds covering complex road junctions. The Photogrammetric Record, 24(125): 23-36 [DOI: 10.1111/j.1477-9730.2008.00516.x]

Poullis C and You S. 2010. Delineation and geometric modeling of road networks. ISPRS Journal of Photogrammetry and Remote Sensing, 65(2): 165-181 [DOI: 10.1016/j.isprsjprs.2009.10.004]

Shen W, Li J, Chen Y H, Deng L and Peng G X. 2008. Algorithms study of building boundary extraction and normalization Based on LIDAR Data. Journal of Remote Sensing, 12(5): 692-698

Sithole G and Vosselman G. 2005. Filtering of airborne laser scanner data based on segmented point clouds. International Archives of Photogrammetry, Remote Sensing and Spatial Information Sciences, 36: 19

Vosselman G. 2003. 3d reconstruction of roads and trees for city modelling // International Archives of Photogrammetry, Remote Sensing and Spatial Information Sciences. Dresden, Germany, 34: 3

Zhang C S. 2004. Towards an operational system for automated updating of road databases by integration of imagery and geodata. ISPRS Journal of Photogrammetry and Remote Sensing, 58(3/4): 166-186 [DOI: 10.1016/j.isprsjprs.2003.09.004]

Zhang R, Zhang J X and Li H T. 2008. Semi-automatic extraction of r ibbon roads from high resolution remotely sensed imagery based on angular texture signature and profile match. Journal of Remote Sensing, 12(2): 224-232

Zhu P, Lu Z, Chen X, Honda K and Eiumnoh A. 2004. Extraction of city roads through shadow path reconstruction using laser data. Photogrammetric Engineering and Remote Sensing, 70(12): 1433-1440

Zuo X Q, Li Q Q and Tang L L. 2004. 3D modeling and data organization of highway. Geomatics and Information Science of Wuhan U niversity, 29(2): 179-183

改进邻域结构与轮廓分析的 LiDAR 点云立交桥提取

陈卓[1] ,马洪超[1,2] ,张良[1]

1. 武汉大学 遥感信息工程学院,湖北 武汉 430079;
2. 武汉大学 测绘遥感信息国家重点实验室,湖北 武汉 430079

摘 要: 由于缺乏有效并具有针对性的方法以及传统遥感影像的 2 维局限性,城市立交桥点的识别与轮廓提取存在较大困难。本文基于机载 LiDAR 点云数据提出一种城市立交桥的提取方法。首先,通过基于局部平面约束的剖面点分割方法,利用多方向扫描线建立改进的剖面邻域点云组织结构,从而提取出立交桥种子点。然后,利用 Alpha-shape 算法定位立交桥轮廓,并获取立交桥初始点。最后,利用区域增长的方法提取出完整结构,同时获取立交桥轮廓。实验结果表明,从提取结果上获取的立交桥长度、宽度以及形态等指标与人工量测结果相近,具有较高的准确度。

关键词: 立交桥,LiDAR,扫描线剖面邻域结构,Alpha-shape 算法

中图分类号: P237 **文献标志码:** A

引用格式: 陈卓,马洪超,张良. 2013. 改进邻域结构与轮廓分析的 LiDAR 点云立交桥提取. 遥感学报,17(5): 1146-1157

Chen Z, Ma H C and Zhang L. 2013. Cloverleaf interchange boundary extraction from airborne LiDAR data based on advanced neighborhood structure and contour analysis. Journal of Remote Sensing, 17(5): 1146-1157 [DOI: 10.11834/jrs.20131213]

1 引 言

城市立交桥作为一种由主体桥面、空间交叉以及空间连接部分等多种构造物组成的多层 3 维地物,是城市交通网络的重要部分,也是城市道路中最复杂的环节(Chen 等,2000; 李卉,2011)。长期以来,对于城市交通的研究大多数是对于道路信息的获取与重建,针对立交桥的信息提取一直缺乏有效的研究成果。从遥感数据中提取立交桥信息迫切需要有效的方法。

传统的道路研究包括从影像或其他数据源中提取道路像素、道路边缘以及估计道路参数(方向、宽度、中心线)的诸多自动或半自动方法(Hu 和 Tao,2007; Poullis 和 You,2010; 林祥国,2012; 张睿等,2008),然而立交桥虽具备一定的道路特点,但同时具有多层次空间复杂结构,所以道路识别中的 2 维方法以及判断依据无法解决问题。Zhang 尝试在轮廓与影像匹配上利用立体测图的方法进行 3 维道路重建,但其方法流程复杂而且无法重建多层结构(Zhang,2004)。左小清等人(2004)将 2 维道路轮廓投影到数字地面模型 DTM(Digital Terrain Model)上,赋予轮廓点 3 维坐标,但作为 3 维道路可视化的一个初步尝试,该文对线面在 3 维环境下的定位和表达没有涉及。机载激光雷达系统(LiDAR 系统)作为一种新型的对地观测传感器,具备在较短时间内迅速获取城市地区的高密度点云的能力(Ackermann,1999),这为具有复杂 3 维结构的地物的信息获取提供了良好条件。在城市交通方面,也出现了一些基于 LiDAR 数据的研究成果(Zhu 等,2004; Clode 等,2006)。在地物 3 维信息提取方面,Vosselman 首先提出了用 LiDAR 数据 3 维信息更新 2 维数据的地物重建方法,并基于地籍图的边缘信

收稿日期:2011-08-15; 修订日期:2013-03-25; 优先数字出版日期:2013-04-02

基金项目:国家科技支撑项目(编号:2012BAH34B02); 武汉大学博士生自主科研项目(编号:2013213020203)

第一作者简介:陈卓(1985—),男,博士研究生,主要研究方向为机载 LiDAR 数据处理与应用理论与技术。E-mail: zchen0916@whu.edu.cn

通信作者简介:马洪超(1969—),男,教授,主要研究方向为 LiDAR 数据处理与应用,遥感图像处理及地统计学。E-mail: hchma@whu.edu.cn

息以及街道、树木的先验知识，提出了多种关于城市地区的街道以及树木的 3 维重建算法及处理流程(Vosselman, 2003)。Oude Elberink 遵循 Vossolmen 的思路，结合 LiDAR 与 map 数据，完成了多层结构的重建，能够提取城市地区立交桥点并重建其 3 维结构(Oude Elberink 和 Vosselman, 2003)，但其在预处理上运用了大量的平面分割与拟合的操作，计算量巨大，其中直线检测的搜索方式在较大曲率结构的立交桥情况下无法适用，且存在 map 数据与 LiDAR 数据的配准问题。

本文首次提出从 LiDAR 点云中提取大型立交桥的方法与流程，在城市密集区数据中提取了立交桥脚点及其轮廓。方法在离散点云上建立了一种改进的扫描线剖面邻域结构(advanced scanline profile neighborhood structure)，能够将属于不同地物的点集分割，形成多个独立连通区域。并通过提取种子点区域 3 维轮廓和分析，识别出立交桥。

2 基于改进邻域结构与轮廓分析的立交桥提取算法

城市立交桥在空间上高于地物表面，而在形态上，除去主体桥之外，还在左、右两侧存在多个曲率较大，高程变化的空间跨桥和分支。本文方法依赖于改进的点云剖面邻域结构的建立，其具备很好的多层次，多平面的分割与识别能力，且能够忽略地物的复杂形状，适用于对城市立交桥的识别。在邻域结构建立之后提出了基于 Alpha-shape 的种子点轮廓提取与筛选策略，保证了边缘轮廓的精确提取以及立交桥点提取的高准确度。最后，利用区域增长的方法提取出完整的立交桥点并重建其轮廓。算法整体流程图如图 1 所示。

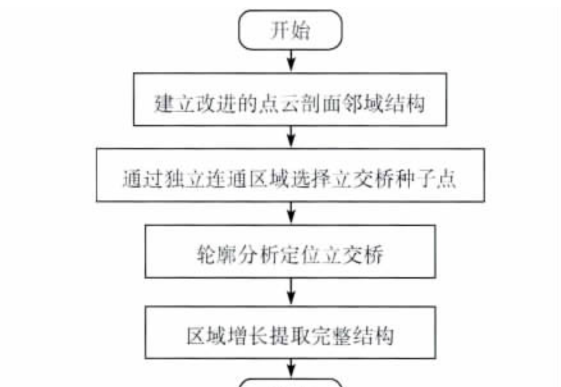

图 1 算法流程

2.1 改进的点云剖面邻域结构

有效的点云数据组织是算法执行的重要部分和基础，而这其中确立点与点之间的邻接关系又是其主要任务(Filln 和 Pfeife, 2005)。常见的点云邻域组织方式包括规则格网(grid)和不规则三角网(TIN)，而内插格网会损失点云的精度，TIN 结构对于边界以及拓扑关系的表达又很模糊。

剖面工具(profile tool)是通过将窄条区域内的点云投影到垂直平面上，直观的查看点云的高程起伏的数据处理工具。Sithole 和 Vosselman(2005)利用这种思想提出建立一种基于剖面的点云邻域结构，以扫描线方式覆盖整个点云，以单个扫描线范围作为剖面区域，将剖面内点集排序，按照坡度阈值确立点与点的邻接关系，如图 2 所示，分割后的点云区段称为链段，如 L_1。整个点云按照不同方向(一般为水平、垂直以及倾斜 45°方向)扫描线分割后相交形成多个独立连通区域。将这一结构用于点云滤波中，可以取得不错的效果，且分割结果与地物本身形态无关，但是单一的阈值判断在不同地物集中的地方容易出现错误的分割，如图 2 中 L_1，L_3，这影响到后续算法的处理。

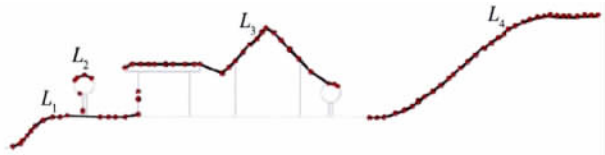

图 2 坡度阈值的分割

在剖面内点集中，不同的地物点一般处于不同的平面上，具有不同的平均坡度值，此外，点集之间的密度也有所差别。为了改进点云邻域结构，避免错误的分割，提出了基于局部平面的分割方法(图 3)。在剖面区域内首先检测多个不同坡度的直线段，并结合密度进行判断，之后对坡度变化平缓的相邻区段进行合并，按照多个方向扫描线形成改进的剖面邻域结构。与之前的结构相比，改进的结构能够更精细的表达点与地物的隶属关系(对于许多不规则地物，如人字形屋顶的建筑物，如图 3 中 L_6，L_7，分割会更加细致)，同时避免了错误的分割，为算法后续的处理提供了重要基础。几种可视化之后的不同点云邻域关系如图 4 所示。建立改进点云邻域结构的具体步骤如下:

(1) 计算落入剖面区域内的数据点集，按照 $X' = x\sin\theta + y\cos\theta$ 值排序(x，y 为数据点坐标，θ 为扫

描线方向角)。对于任意数据点 P_i,计算其与前一位置数据点 P_{i-1} 的坡度 $S(P_{i-1},P_i) = \arctan\left(\frac{z_i - z_{i-1}}{\sqrt{(x_i - x_{i-1})^2 + (y_i - y_{i-1})^2}}\right)/\pi$,$z_i$ 为高程值,利用直方图统计点的坡度信息,统计间隔为 $5/\pi$。

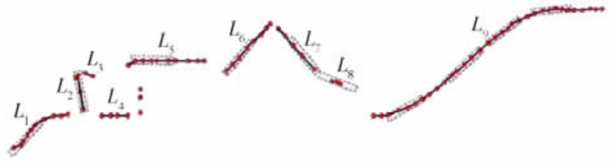

图3　基于局部平面的剖面链分割

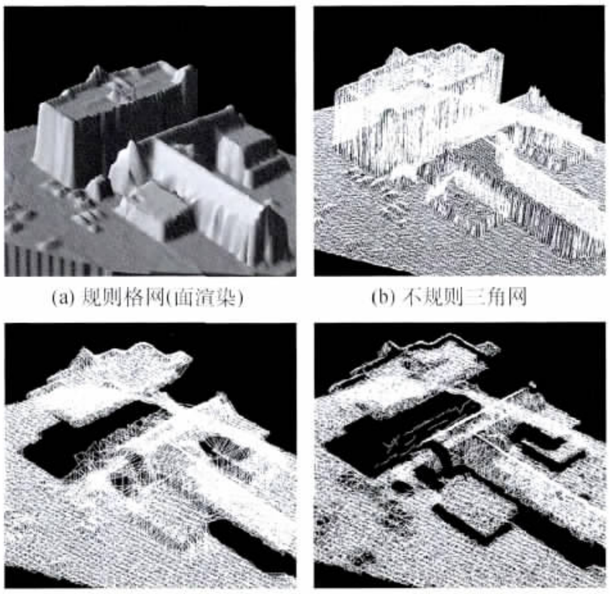

(a) 规则格网(面渲染)　(b) 不规则三角网

(c) 剖面邻域结构(坡度分割)　(d) 改进的剖面邻域结构

图4　点云领域结构可视化

(2) 依次获取累计数目大于 2 的区间内点集 $\boldsymbol{G}_i = \{P_0,\cdots,P_i\}$。随机选取 P_j,若 $P_{j-1},P_{j+1} \in \boldsymbol{G}_i$ 则将 $\{P_{j-1},P_j,P_{j+1}\}$ 作为链段 L_1 的初始点,连接相邻位置点并计算 L_1 的平均点间距 D_{a1},点间距均方差 δ_1 以及平均坡度 S_{a1},同时对 L_1 内的点集拟合直线 l_1。

(3) 以直线 l_1 为中心轴,构建半径为 R 的空间圆柱体区域。分别搜索 L_1 两端的前、后一位置点 P_{j-2},P_{j+2}。若 P_{j-2} 和 P_{j-1} 的距离 $|D_{j-2,j-1} - D_{a1}| < 3\delta_1$ 或 $|D_{j+1,j+2} - D_{a1}| < 3\delta_1$ 且点 P_{j-2} 或 P_{j+2} 落入圆柱体区域内,则将 P_{j-2} 或 P_{j+2} 加入到链段 L_1 中,更新平均间距及方差并重新拟合直线 l_1。若不满足条件,则对 P_{j-3} 或 P_{j+3} 进行同样判断,满足条件则加入到 L_1 点集中,将 P_{j-2} 或 P_{j+2} 视作孤立点,否则停止该端的搜索。完成链段 L_1 的搜索后,将 L_1 中的点从 $\boldsymbol{G}_i$ 中删除,搜索新的链段。重复步骤(3),直到 $\boldsymbol{G}_i$ 中的点数少于 2。

(4) 遍历剖面区域内的链段集合,若两个相邻链段 L_i,L_j 之间,L_i 的末节点与 L_j 的首节点之间距离满足 $D_{ei,hj} < \max(D_{ai},D_{aj}) + 3\max(\delta_i,\delta_j)$,计算 L_i 和 L_j 的相似系数 $\text{sim}_{i,j} = \frac{1}{1 + \sqrt{(D_{ai} - D_{aj})^2 + \beta(S_{ai} - S_{aj})^2}}$,$\beta$ 为调节参数,用来统一平均坡度与点间距的度量以及调整两者对于相似性影响的权重。若 $\text{sim}_{i,j}$ 小于阈值 $\min_{\text{sim}}$,则将 L_i,L_j 合并。重复步骤(4),直到集合内没有可以合并的相邻链段。

算法执行中,扫描线宽度应与点云平均间距相同,保证区域内的点云宽度为 1。在点集分割的过程中,距离判断式里 3 倍均方差 δ 为数据处理中同类数据判断的经验值。

2.2　种子点选取

根据城市地区立交桥所具有的多种特点以及 LiDAR 系统特性对立交桥描述如下:(1) 空间上,立交桥点是城市道路的 3 维空间延伸,其主桥及所有支路部分均位于地面以上。(2) 形态上,大型立交桥一般横跨较长的路段,所以在其区域内存在的最长链段长度应大于其他地物,如建筑物和植被。(3) 立交桥主桥的端点与支路部分的末尾与地面平缓相连,其接口处的桥面方向与相接的道路方向平行,立交桥模型如图 5 所示。

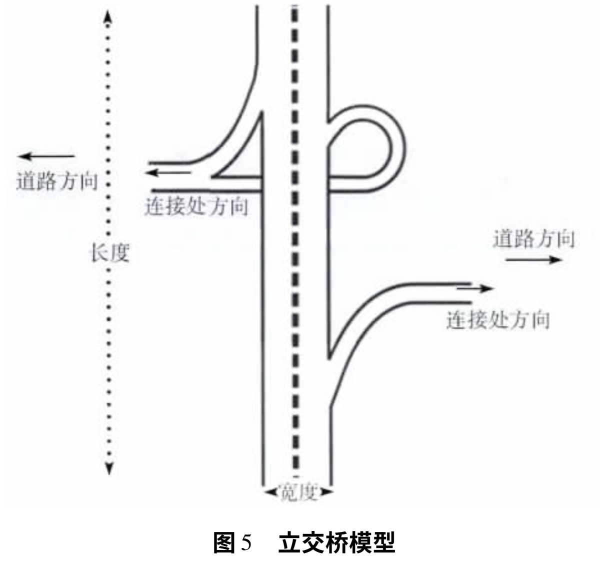

图5　立交桥模型

基于 2.1 节的点云组织方法,依据描述(1),从点云数据中提取种子点如下:

首先定义分割的高程差阈值 Δ_{upper}。然后,取同一剖面链分割形成的链段集合 $\{L_1,L_2,\cdots,L_i\}$,若对于链段 L_i,其点集 $\boldsymbol{PS}_i$ 的每一个点高程 H_{P_i} 与相邻

链段点集的平均高程 $H_{L_{i-1}}$，$H_{L_{i+1}}$ 比较有 $H_{P_i} - \min(H_{L_{i-1}}, H_{L_{i+1}}) > \Delta_{\text{upper}}$，则将 L_i 标记为 upper 链段。若集合中 L_j 与 upper 链段 L_i 相邻，且 $\left|H_{L_i} - H_{L_j}\right| < \Delta_{\text{upper}}$，则将 L_j 也标记为 upper 链段。最后，对于点云数据 $N_{\text{LAS}}(P)$ 中的每一个数据点 P_i，计算经过该点的不同方向的链段集合 $\boldsymbol{G}_i = \{L_1, L_2, \cdots, L_n\}$ ($n <$ 扫描方向数) 与 upper 链段的个数 $Num_{\text{upper}}(\boldsymbol{G}_i)$，种子点集 $\boldsymbol{N}_{\text{Seed}}(P) = \{P_i \in \boldsymbol{N}_{\text{LAS}}(P) \mid Num_{\text{upper}}(\boldsymbol{G}_i) \geqslant Num(G_i)/2\}$。如图 6 中点 1，点 3，点 4，点 5，算法可用于多层结构(点 5) 且在多种地物形状下(点 1，点 3，点 4) 同样适用。

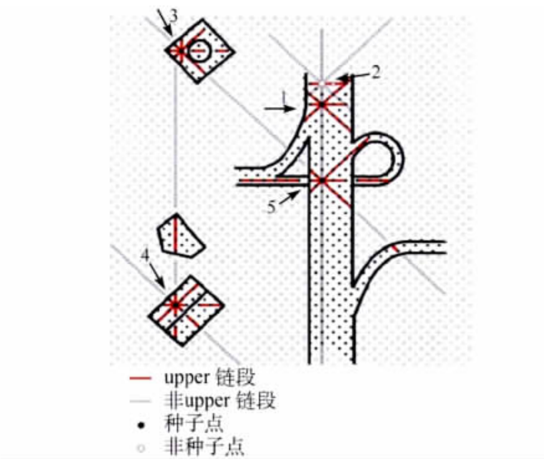

图 6　种子点提取

2.3　轮廓筛选与完整结构提取

在提取的种子点中，需要通过分析区域轮廓，结合立交桥模型描述进行种子点筛选。然而常规的凸包算法对于不规则边缘的点集无法求取精确轮廓，且无法在多个点集之间进行分割(图 7(a))，这阻碍了算法的进一步处理。本文提出基于 Alpha-shape 的种子点轮廓提取与筛选策略，从而能够保留正确的立交桥脚点。

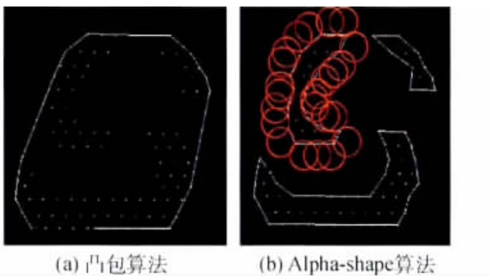

图 7　种子点轮廓提取

Alpha-shape 算法的优势在于可以重建无序点集的精确边缘，其原理可以比作一个半径为 alpha 的圆在点集外部滚动，如果存在空洞与间隙大于 alpha 值，还可以滚动到点集内部，将其分割为多个独立子集，滚动的轨迹是各个子集的精确边缘(图 7(b))(沈蔚 等，2008)，这刚好能满足种子点的区域分割和轮廓筛选的要求。轮廓分析的具体步骤如下:

(1) 分离种子点与非种子点，利用 k 均值聚类算法与点的连通性去除孤立点、噪声点以及远离聚类中心的个别点。

(2) 利用 Alphas-shape 求出种子点轮廓，形成分割后的种子点轮廓集 $\alpha\text{-}Shape = \{\boldsymbol{A}_1, \boldsymbol{A}_2, \cdots, \boldsymbol{A}_n\}$，$\boldsymbol{A}_i$ 为轮廓。

(3) 轮廓 $\boldsymbol{A}_i$ 有首尾相连的多条边组成 $\boldsymbol{A}_i = \{E_1, E_2, \cdots, E_n\}$，将组成轮廓的边 E_i 分为两类，定义阈值 Δ_{junc}，沿此边的方向在 E_i 左右建立等面积的矩形缓冲区，计算落入两侧缓冲区的点集平均高程之差 H_{Diff}，若 $H_{\text{Diff}} < \Delta_{\text{junc}}$，则将 E_i 标记为 Junction 边，否则将其标记为 Common 边。

(4) 在 $\alpha\text{-}Shape$ 中，排除掉所有不含有 Junction 边的轮廓(如图 8 左侧的多个轮廓)，在余下的轮廓集中，依据描述(2) 选取在轮廓区域内含有最长链段的轮廓作为立交桥初始轮廓，轮廓内所有点为提取的初始立交桥点。

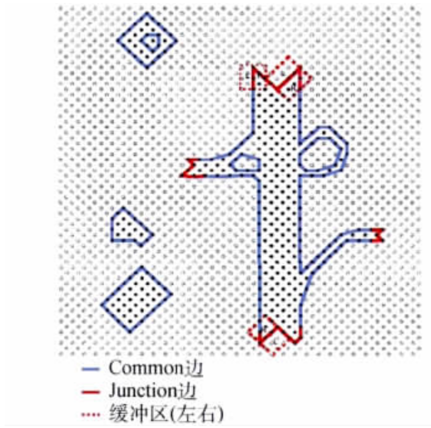

图 8　轮廓筛选

在初始点中大部分立交桥点已经提取，但在与地面的接口处尚不完整，这是因为在接口处点所在的某些方向的链段已经和地面点相连，不属于 upper 链段。本文利用区域增长的方法提取出完整结构。获取所有 Junction 边的端点作为区域生长的初始点。针对点集中每一个点，计算穿过该点的非 upper 链段的长度，取多数点的最大长度链段的方向为接口所在的道路方向。依据描述(3) 将此方向作为区域生长的方向。获取点集中数据点所在链段的后继

点 P_i,以前、后点为中心拟合直线 $line_{i-}$,$line_{i+}$,如图9,并比较线拟合差 $Diff_-$,$Diff_+$,若 $Diff_- \leqslant Diff_+$,则将其加入立交桥点集,重复操作直到不满足条件的点出现。

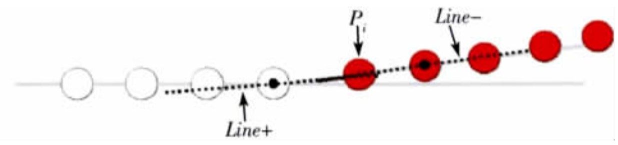

图9 区域增长-直线拟合差比较

3 实验与分析

为了验证本文算法的可行性与有效性,采用2009年南宁市区的机载LiDAR数据进行实验。试验平台采用自主开发的ALDPro软件平台。试验数据中采集于城市中心建筑密集区,包含了大型立交桥、城市主要交通干道以及多种城区地物,如图10(a)。经过多次试验和反复验证,采用以下参数值可以取得满意的效果,如表1。其中upper链段和Junction边的判断阈值可由人工设定,并在一定范围内对提取结果影响不大,Alpha-shape半径参数取略大于平均点密度的值。

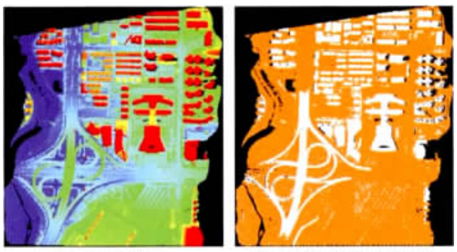

(a)点云数据 (b)种子点提取结果

图10 种子点提取

表1 算法参数

参数	参数说明	实验取值
$\min_{sim}$	相似系数最小值	0.74
β	相似系数调节参数	0.11
Δ_{upper}	upper链段高程差阈值	2.47 m
Δ_{junc}	Junction边判断阈值	1.52 m
α	Alpha-shape半径参数	2.80 m

图10(b)表示种子点提取的结果,种子点包括了立交桥脚点、建筑物,植被等,可以看出基于改进结构的种子点子集划分更加明确,提取结果较为完整。图11(a)为除掉孤立点之后,Alphas-shape方法求取的种子点轮廓,可以看到,方法能够对子集进行分割并精确的求取其轮廓。

(a)种子点轮廓提取与筛选 (b)立交桥点

图11 立交桥点提取

图11(b)表示轮廓筛选后立交桥脚点的提取,包括主桥面点以及所有支路,但在A、B、C 3处存在不完整的问题,图12(a)表示区域增长后提取的完整结构。图12(b)表示本文提取的完整的立交桥轮廓。

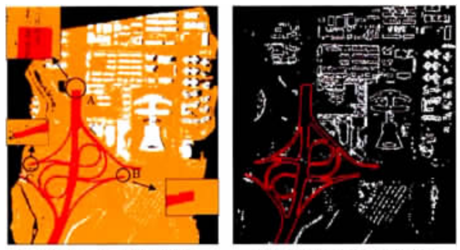

(a)完整立交桥脚点 (b)完整立交桥轮廓

图12 立交桥完整提取

为了验证提取方法的完整性,给出一种定量分析的指标,将提取结果与人工分类的结果进行比较,本文方法所提取的立交桥点数为42367个点,而人工分类的立交桥点为44352个点,经过分析方法的完整度达到92.94%。此外,方法的一类误差率(弃真)为4.47%,主要来源于已与路面相接的道路接口处未被分割与识别部分。二类误差率(纳伪)为2.75%,主要来源于桥面上行驶的少量车辆点。还将提取后的立交桥主桥、支路中心线的长度以及路面宽度与0.3 m正射影像上叠加进行对比,如图13。经过对比发现,在大部分地区本文方法所提取的立交桥轮廓与正射影像中标识的边缘相差在1—2个像素之间,大部分来自于点云采样和图像网格之间的差异(图13(b))。而在局部地区(如图13(c)),由于受树木遮挡点云存在较大空洞,误差较大,目测在3—4个像元左右。

影响提取完整性另一部分原因主要包括:由于少数桥面边缘的扶手点、主桥中心的隔离带点因与周围平面高程相差较大,被视作孤立点滤除;数据边缘形成的空洞也在一定程度上影响了区域增长算

法; 墙面上存在多个数据点,因 X' 值相同无法进行排序,导致墙面点集无法正确分割。

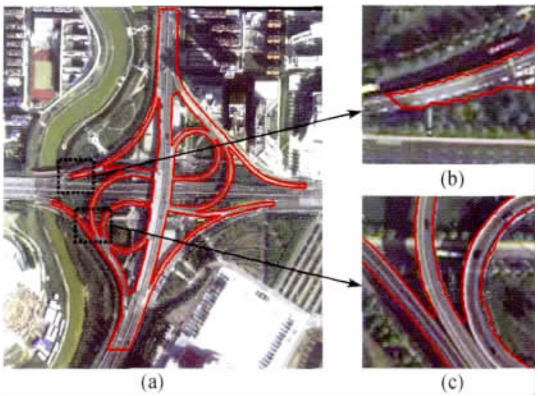

图 13 与正射影像叠加显示

4 结 论

本文首次提出并实现的方法可以自动、完整地提取 LiDAR 数据中的立交桥脚点,同时精确提取立交桥轮廓。提出了基于局部平面的剖面点集分割方法,建立了改进的剖面邻域的点云组织结构,实现了不同地物点集的精细分割,避免了单一阈值判断出现的错误,并提取立交桥种子点。提出基于 Alpha-shape 的种子点轮廓筛选策略,能够精确的提取立交桥的不规则轮廓,提高了提取算法的准确度。实验证明,本文算法提取立交桥具有较高的完整性,在提取轮廓上精度较高,是可行的、有效的。其结果可在立交桥形态设计、数字城市建设与交通信息管理上发挥重要作用。桥面与地面接口处的提取完整度有待提高,需要在点云中加入桥面车辆点的识别,进一步减小二类误差。此外,需要研究有效的立交桥轮廓简化算法,消除轮廓所存在的毛刺和严重的凹陷。

参考文献(References)

Ackermann F. 1999. Airborne laser scanning-present status and future expectations. ISPRS Journal of Photogrammetry and Remote Sensing, 54(2/3): 64 – 67 [DOI: 10.1016/S0924 – 2716(99)00009 – X]

Chen J, Sun M and Zhou Q M. 2000. Expression and visualization of cloverleaf junction in a 3-dimensional city model. GeoInformatica, 4(4): 375 – 386 [DOI: 10.1023/A:1026513912425]

Clode S, Rottensteiner F, Kootsookos P J and Zelniker E E. 2006. Detection and vectorisation of roads from lidar data. Photogrammetric Engineering & Remote Sensing, 2006

Filin S and Pfeifer N. 2005. Neighborhood systems for airborne laser data. Photogrammetric Engineering & Remote Sensing, 71(6): 743 – 755

Hu X and Tao V. 2007. Automatic extraction of main road centerlines from high resolution satellite imagery using hierarchical grouping. Photogrammetric Engineering and Remote Sensing, 73: 1049 – 1056

李卉. 2011. 集成 LiDAR 和遥感影像城市道路提取与三维建模. 测绘学报, 40(1): 133

林祥国. 2012. 高分辨率遥感影像道路半自动追踪方法研究. 测绘学报, 41(4): 631

Oude Elberink S J and Vosselman G. 2009. 3D information extraction from laser point clouds covering complex road junctions. The Photogrammetric Record, 24(125): 23 – 36 [DOI: 10.1111/j.1477 – 9730.2008.00516.X]

Poullis C and You S. 2010. Delineation and geometric modeling of road networks. ISPRS Journal of Photogrammetry and Remote Sensing, 65(2): 165 – 181 [DOI: 10.1016/j.isprsjprs.2009.10.004]

沈蔚, 李京, 陈云浩, 邓磊, 彭光雄. 2008. 基于 LIDAR 数据的建筑轮廓线提取及规则化算法研究. 遥感学报, 12(5): 692 – 698

Sithole G and Vosselman G. 2005. Filtering of airborne laser scanner data based on segmented point clouds. International Archives of Photogrammetry, Remote Sensing and Spatial Information Sciences, 36: 19

Vosselman G. 2003. 3d reconstruction of roads and trees for city modelling // International Archives of Photogrammetry, Remote Sensing and Spatial Information Sciences. Dresden, Germany, 34: 3

Zhang C S. 2004. Towards an operational system for automated updating of road databases by integration of imagery and geodata. ISPRS Journal of Photogrammetry and Remote Sensing, 58(3/4): 166 – 186 [DOI: 10.1016/j.isprsjprs.2003.09.004]

张睿, 张继贤, 李海涛. 2008. 基于角度纹理特征及剖面匹配的高分辨率遥感影像带状道路半自动提取. 遥感学报, 12(2): 224 – 232

Zhu P, Lu Z, Chen X, Honda K and Eiumnoh A. 2004. Extraction of city roads through shadow path reconstruction using laser data. Photogrammetric Engineering and Remote Sensing, 70(12): 1433 – 1440

左小清, 李清泉, 唐炉亮. 2004. 公路三维模型建立与数据组织. 武汉大学学报(信息科学版), 29(2): 179 – 183